JCTC Journal of Chemical Theory and Computation

A Fast Implementation of Perfect Pairing and Imperfect Pairing Using the Resolution of the Identity Approximation

Alex Sodt, Greg J. O. Beran, Yousung Jung, Brian Austin, and Martin Head-Gordon

Department of Chemistry, University of California, Berkeley, and Chemical Sciences Division, Lawrence Berkeley National Laboratory, Berkeley, California 94720-1460

Received September 22, 2005

Abstract: We present an efficient implementation of the perfect pairing and imperfect pairing coupled-cluster methods, as well as their nuclear gradients, using the resolution of the identity approximation to calculate two-electron integrals. The perfect pairing and imperfect pairing equations may be solved rapidly, making integral evaluation the bottleneck step. The method's efficiency is demonstrated for a series of linear alkanes, for which we show significant speed-ups (of approximately a factor of 10) with negligible error. We also apply the imperfect pairing method to a model of a recently synthesized stable singlet biradicaloid based on a planar Ge−N−Ge−N ring, confirming its biradical character, which appears to be remarkably high.

1. Introduction

Resolution of the identity (RI) or density fitting (DF) methods trace their lineage back to early attempts to approximate two-center, four-electron integrals.[1−3] For example, as early as 1939, Sklar used bond-centered auxiliary functions to simplify integral evaluation in an analysis of benzene.[1] In 1966, Harris and Rein approximated two-center function products as sums of one-center function products, determining the auxiliary expansion coefficients by fitting Coulomb integrals, rather than by an overlap criterion.[4] In 1971, Billingsley and Bloor approximated two-center AB products with a linear combination of functions centered on A and B, using what is essentially the procedure we use today: inverting the auxiliary basis Coulomb interaction matrix.[5] In 1969, Newton[6] and, in 1973, Baerands et al.,[7] performed a least-squares fit of the density for their self-consistent field (SCF) calculations, which is now termed[8] the "**S**" approximation, as it effectively minimizes the squared deviation in the overlap (an overlap matrix typically is called an **S** matrix) of the density minus its fit. Also in 1973, Whitten provided theorems bounding the error of least-squares integral fitting, in the Coulomb metric.[9]

In 1979, Dunlap et al. performed a bounded fit of the density for use in $\chi\alpha$. calculations.[10] They minimized the Coulomb self-repulsion of the density minus its fit, a positive semidefinite quantity. They term bounded fits of this nature to be "robust", an adjective we consider to be apt. Dunlap concluded that fitting the electric field generated by electrons is better than fitting the electron density, in the sense that it eliminates first-order error in the fit.[10] This is now termed the "**V**" approximation, where **V** typically denotes an inner product of the Coulomb operator.[8]

Toward applying the RI approximation for general two-electron fitting (rather than fitting a density), which would be useful for correlated wave function theories, Vahtras et al. performed numerical tests of both the **S** and **V** approximations. They found that the **V** approximation reproduced the SCF energy quite accurately, even for modestly sized auxiliary basis sets.[8]

In 1995, Eichkorn et al. produced an auxiliary basis set which reproduced the **J** matrix to reasonable accuracy, with an auxiliary basis set of approximately 3 times the size of the orbital basis set.[11] Optimized basis sets for use with MP2 followed,[12,13] which were able to reproduce results within a few μH per atom.

One expects such success from this density fitting procedure because, while the linear combination of atomic orbitals (LCAO) basis set (denoted by greek indices) used might not be very linearly dependent, the product space (termed $\mu\nu$ products) almost certainly will be.[14,15] This two-center

10.1021/ct050239b CCC: $33.50
Published on Web 01/11/2006

product space is then very amenable to an expansion in a much smaller basis (or perhaps by simply eliminating the linearly dependent portion of the space outright[14−16]).

The computational advantage of the RI approximation is not only that it reduces the four-center integrals to a composite of three-center ones but also that it separates the two-electron integral into a contraction over two one-electron expansions, which can be transformed to a molecular orbital representation independently. It is, thus, an indispensable tool for methods limited both by integral computation (such as Hartree−Fock theory[17]) and by temporary storage for the atomic orbital (AO) to molecular orbital (MO) transformation (such as MP2).[18] The RI method has some similarities with the pseudospectral method, which has also been implemented for perfect pairing[19] (PP). Relative to the pseudospectral approach, RI methods have the advantage of being completely smooth and, thus, so too are the potential energy surfaces that result.

We apply the RI approximation to perhaps the most basic of correlated wave function methods, PP[20,21] and imperfect pairing (IP), which are described in more detail elsewhere.[22−24] Both of these methods can be viewed as approximations to valence-optimized doubles (VOD),[25] itself an approximation to a complete valence space treatment, complete active space−self-consistent field (CASSCF). VOD represents a triumph in that it scales to the sixth order (as opposed to exponential scaling, like CASSCF), yet even sixth-order scaling practically imposes a hard wall beyond which we cannot apply the method.

In coupled-cluster theory, the ground-state trial wave function is written as an exponentiated excitation operator acting on a reference state, $|0\rangle$:

$$|\Psi\rangle = \exp(\hat{T})|\,0\rangle \tag{1}$$

where, for VOD, the $\hat{T}$ operator is

$$\hat{T}_{\mathrm{VOD}} = \sum_{ijk^*l^*} t_{ij}^{k^*l^*} a_{k^*}^{\dagger} a_{l^*}^{\dagger} a_j a_i \tag{2}$$

The orbital occupation creation and annihilation operators ($a^{\dagger}$ and a, respectively) are weighted by so-called t amplitudes, t.

PP truncates the excitation operator to include what would presumably be the most important double excitations. Each active α electron is paired with exactly one β electron, and they are simultaneously correlated with exactly one pair of virtual orbitals. In this way, pairs of electrons are correlated independently of each other. The form of the PP excitation operator is

$$\hat{T}_{\mathrm{PP}} = \sum_i t_{i\bar{i}}^{i^*\bar{i}^*} a_{i^*}^{\dagger} a_{\bar{i}^*}^{\dagger} a_{\bar{i}} a_i \tag{3}$$

This operator should perform well for breaking isolated bonds; as occupied and virtual orbitals become nearly degenerate, the PP wave function will be able to contain a mixture of the two.

IP truncates the coupled-cluster doubles (CCD) excitation operator such that correlation is provided between the most important pairs. IP allows one electron to be excited from each of two pairs simultaneously. The form of the IP excitation operator for a system with an even number of electrons is

$$\hat{T}_{\mathrm{IP}} = \hat{T}_{\mathrm{PP}} + \sum_{i\neq j}\left(t_{i\bar{j}}^{i^*\bar{j}^*} a_{i^*}^{\dagger} a_{\bar{j}^*}^{\dagger} a_{\bar{j}} a_i + t_{i\bar{j}}^{i^*\bar{i}^*} a_{j^*}^{\dagger} a_{\bar{i}^*}^{\dagger} a_{\bar{j}} a_i + \frac{1}{2} t_{ij}^{i^*j^*} a_{i^*}^{\dagger} a_{j^*}^{\dagger} a_j a_i + \frac{1}{2} t_{\bar{i}\bar{j}}^{\bar{j}\bar{i}^*} a_{\bar{j}^*}^{\dagger} a_{\bar{j}^*}^{\dagger} a_{\bar{j}} a_{\bar{i}} \right) \tag{4}$$

This operator retains the desirable properties of PP, yet will also correlate important open-shell configurations. It also provides interpair correlation, which is physically important in cases such as multiple bonding. Also, for systems that do not resemble a group of localized electron pairs, it will provide a more physically consistent description than PP. Van Voorhis and Head-Gordon explained this illustrative example in their development of IP: Benzene's π electrons are completely delocalized across the six-membered ring. Instead of selecting delocalized correlating orbitals that reflect this, PP instead localizes the electrons to maximize the pair correlation. The extra flexibility granted to IP remedies this problem to a large extent, but there is still spurious symmetry breaking as the method still places too much emphasis on the most important pair excitations.[23]

The coupled-cluster equations are solved iteratively, in a process which, for a full doubles treatment, scales to the sixth power of system size (o^2v^4). In contrast, the effect of the limited number of PP and IP amplitudes is to make two-electron integral construction (scaling to the fourth power of system size) more expensive than actually solving the equations (for IP, this scales to the third power of the number of pairs, while in PP, the amplitudes are independent of each other). While the integrals are limited in number, they must still be formed from many integrals over atomic orbitals. It is just such a case for which the RI approximation should prove most successful; it provides a total reduction in the number of base integrals computed, and it may transform each electron of the two-electron integral independently.

The PP and IP orbitals are optimized such that they provide the lowest total energy (this also serves to define a unique pairing scheme). This is accomplished by forming the gradient of the energy with respect to orbital rotation and then performing standard search techniques to minimize the energy. Taking this orbital gradient requires an expanded set of Coulomb integrals, all of which can be obtained from the following half-transformed integrals:[19,22]

$$\begin{gathered}
\mathbf{J}_{\mu\nu}^{ii} = (ii|\mu\nu) \\
\mathbf{J}_{\mu\nu}^{ii^*} = (ii^*|\mu\nu) \\
\mathbf{J}_{\mu\nu}^{i^*i^*} = (i^*i^*|\mu\nu) \\
\mathbf{K}_{\mu\nu}^{ii} = (i\mu|i\nu) \\
\mathbf{K}_{\mu\nu}^{ii^*} = (i\mu|i^*\nu) \\
\mathbf{K}_{\mu\nu}^{i^*i^*} = (i^*\mu|i^*\nu)
\end{gathered} \tag{5}$$

2. Algorithm

In developing an RI approximation for computing these intermediates, we first define the auxiliary basis expansion of a single function product, $|\mu\nu)$. We minimize the self-interaction of the product minus its fit:

$$(\mu\nu - \overline{\mu\nu}|\mu\nu - \overline{\mu\nu}) \tag{6}$$

This leads to the following (optimal[26]) expression for the four-center two-electron integrals in terms of a set of three-center quantities, the **B** tensors, which are given both in terms of atomic orbitals (Greek letters) and in auxiliary basis functions (L, M...):

$$(\mu\nu|\lambda\sigma) \approx \sum_L \mathbf{B}^L_{\mu\nu}\mathbf{B}^L_{\lambda\sigma} = \sum_{LMN}(\mu\nu|L)(L|M)^{-1/2}(M|N)^{-1/2}(N|\lambda\sigma) \tag{7}$$

where a **B** tensor[12] is defined to be

$$\mathbf{B}^L_{\mu\nu} = \sum_K (\mu\nu|K)(K|L)^{-1/2} \tag{8}$$

and where $\mu\nu$ need not necessarily be atomic orbitals but could, in fact, be transformed into molecular orbitals. By expanding two-center functions in terms of one-center auxiliary functions, explicit four-center integrals are never needed. The number of two-center function products, which we call NFP, formally scales linearly with system size, due to the fact that Gaussian AOs have limited spatial extent, and therefore, the product of two well-separated AOs will be negligible. Thus, the number of required two-electron integrals will be reduced, but will still scale quadratically with system size. The task is, thus, to form the requisite **B** tensors most efficiently and, then, to transform them into the **J** and **K** matrices. The following is an outline of the RI algorithm, with the scaling of the step indicated in parentheses.

1a*. Form: $(L|M)^{-1/2}$ (X^3)

2a*. Form: $(\mu\nu|M)$ (NFP X)

3a*. Contract: $\mathbf{B}^L_{\mu\nu} = \sum_M (\mu\nu|M)(M|L)^{-1/2}$ (NFP X^2)

4a. Contract: $\mathbf{B}^L_{\mu[i,i^*]} = \sum_\nu \mathbf{B}^L_{\mu\nu}C_{\nu[i,i^*]}$ (NFP $X\,o$)

5a. Contract: $\mathbf{B}^L_{[ii,ii^*,i^*i^*]} = \sum_\mu \mathbf{B}^L_{\mu[i,i^*]}C_{\mu[i,i^*]}$ ($X\,N\,o$)

6a. Contract: $\mathbf{K}^{[ii,ii^*,i^*i^*]}_{\mu\nu} = \sum_L \mathbf{B}^L_{\mu[i,i^*]}\mathbf{B}^L_{\nu[i,i^*]}$ ($X\,N^2\,o$)

7a. Contract: $\mathbf{J}^{[ii,ii^*,i^*i^*]}_{\mu\nu} = \sum_L \mathbf{B}^L_{\mu\nu}\mathbf{B}^L_{[ii,ii^*,i^*i^*]}$ (NFP $X\,o$)

Steps marked with an asterisk need only be computed once per calculation, otherwise the step must be done each time MOs are updated. Comma-separated indices in square brackets are independent, and their contributions to the total cost of the step are, therefore, mutually additive. Contrast this with the alternative algorithm for creating the **J** and **K** matrices using four-center AO integrals without the RI approximation:

1b. Form: $(\mu\nu|\lambda\sigma)$ (NFP^2)

2b. Contract: $\mathbf{K}^{[ii,ii^*,i^*i^*]}_{\mu\nu} = \sum_{\lambda\sigma}(\mu\lambda|\nu\sigma)C_{\lambda[i,i^*]}C_{\sigma[i,i^*]}$ $(\mathrm{NFP}^2\cdot o)$

3b. Contract: $\mathbf{J}^{[ii,ii^*,i^*i^*]}_{\mu\nu} = \sum_{\lambda\sigma}(\mu\nu|\lambda\sigma)C_{\lambda[i,i^*]}C_{\sigma[i,i^*]}$ $(\mathrm{NFP}^2\cdot o)$

Our RI algorithm formally scales with the fourth power of system size (step 6a), while without the RI approximation, the algorithm scales only with the third power of system size (steps 2b and 3b). However, for systems of a size for which either algorithm might be feasible, few function products can be neglected. NFP is, thus, comparable to N^2, yielding effectively fifth-order scaling without the RI approximation. In fact, step 4a of the RI algorithm is the dominant step for small to modestly large systems, both because of the size of NFP and because step 6a is implemented as a matrix multiply, employing optimized standard routines. Step 4a cannot be simply computed as a matrix multiply without breaking the inherent sparsity of the function product. Each step of the RI algorithm may be broken up such that it can be computed using limited memory that scales quadratically with system size. Mass storage requirements scale cubically with system size. Contrast these modest requirements with the coupled-cluster doubles methods that do not employ local truncations, which have large (quartic) disk requirements and large (sixth-order) computational requirements.

We implemented these methods into a development version of the quantum chemistry package, Q-CHEM.[27]

A comparison of the performance of RI−PP, RI−IP, PP, and IP is shown in Table 1. It is evident that the resolution of the identity approximation reduces computation time by approximately one order of magnitude. Also, because the bottleneck step of both PP and IP is the construction of the same integral intermediates, they are both accelerated to the same degree, and indeed, there is little difference in the computational requirements between the methods. The effect of the RI approximation is more pronounced in the larger basis set because the auxiliary basis size does not increase

Table 1. Total CPU Times Comparing Resolution of the Identity (RI) Algorithms for the PP and IP Methods, against a Non-RI PP Algorithm on Linear Alkanes[a]

chain length (basis)	RI−PP CPU (s)	RI−IP CPU (s)	PP CPU (s)	IP CPU (s)
2 (cc-pVDZ)	8.0	8.8	25.0	32.5
2 (cc-pVTZ)	321.3	342.1	1267.6	1373.2
4 (cc-pVDZ)	54.1	63.2	281.1	344.5
4 (cc-pVTZ)	2644.7	2809.7	20688.1	22216.2
6 (cc-pVDZ)	170.4	198.7	1120.1	1564.6
8 (cc-pVDZ)	321.1	402.6	3061.8	4321.6

[a] Calculations were performed using a single 2.3 GHz IBM 970fx processor in an Apple XServe. The basis set used is cc-pVDZ with its RI-MP2 fitting basis.[28] Each calculation required between 11 and 13 iterations.

proportionally with the size of the AO basis. Larger basis sets should be relatively easier to fit, because the linear dependence of the product space ($\mu\nu$) will be greater.

The RI approximation introduces very little error to the PP and IP methods. As an example, for the molecules of the G2 set using the SV[29] basis, the RI approximation (using the algorithm described above) introduces a root-mean-square (RMS) error of 29 μH to the PP energy, or 8 μH per atom. The accuracy of the method is fairly uniform over the set of molecules, the greatest error being 31 μH per atom. For the closed-shell subset of the G2 set, RI−IP gives an RMS error of 64 μH, or 13 μH per atom. The largest error for RI−IP is 71 μH per atom.

3. Nuclear Gradient

In PP and IP, the nuclear gradient is formed from a similar set of intermediate integrals as the orbital gradient:

$$\mathbf{J}^{ii(x)}_{\mu\nu} = (ii|\mu^{(x)}\nu) + (ii|\mu\nu^{(x)})$$
$$\mathbf{J}^{ii^*(x)}_{\mu\nu} = (ii^*|\mu^{(x)}\nu) + (ii^*|\mu\nu^{(x)})$$
$$\mathbf{J}^{i^*i^*(x)}_{\mu\nu} = (i^*i^*|\mu^{(x)}\nu) + (i^*i^*|\mu\nu^{(x)})$$
$$\mathbf{K}^{ii(x)}_{\mu\nu} = (i\mu^{(x)}|i\nu) + (i\mu|i\nu^{(x)})$$
$$\mathbf{K}^{ii^*(x)}_{\mu\nu} = (i\mu^{(x)}|i^*\nu) + (i\mu|i^*\nu^{(x)})$$
$$\mathbf{K}^{i^*i^*(x)}_{\mu\nu} = (i^*\mu^{(x)}|i^*\nu) + (i^*\mu|i^*\nu^{(x)}) \quad (9)$$

The RI algorithm for constructing these integrals follows directly from the RI algorithm above, but acting on six sets of integrals, with *x*, *y*, and *z* derivatives with respect to the center of both μ and ν. However, one must also consider the effect of nuclear displacement on the auxiliary basis function centers. Here is the nuclear gradient of the energy:

$$E^{(x)} = E_0^{(x)} + \sum_i (f_i^{i(x)}\gamma_i^i + f_{i^*}^{i^*(x)}\gamma_{i^*}^{i^*}) + \sum_{pqrs}\Gamma_{pqrs}(pq|rs)^{(x)}_{RI} \quad (10)$$

where the two-electron integral contracted with the effective two-particle density matrix, Γ, is fit using the RI approximation, and the sum over orbitals (*p*, *q*, *r*, and *s*) is restricted to those relevant to the pairing method used.

Derivatives with respect to regular basis function centers are included in the **J** and **K** terms described above. We begin by stating this useful identity for computing derivatives with respect to auxiliary basis centers:

$$\frac{\partial}{\partial x}(K|L)^{-1} = -\sum_{M,N}(K|M)^{-1}\left[\frac{\partial}{\partial x}(M|N)\right](N|L)^{-1} \quad (11)$$

We use the following intermediates for efficiently constructing the gradient:

$$\tilde{\Gamma}^L_{pq} = \sum_{rs,L}(L|M)^{-1}(M|rs)\Gamma_{pqrs} \quad (12)$$

The result is then added to the gradient (the subscript RI indicates that this is only the contribution from the gradient with respect to auxiliary basis center):

$$\tilde{\Gamma}^{KL} = -\sum_{pq}(pq|M)(M|K)^{-1}\tilde{\Gamma}^K_{ab} \quad (13)$$

$$E^{(x)}_{RI} = 2\sum_{pq,K}(pq|K^{(x)})\tilde{\Gamma}^K_{ab} + 2\sum_{KL}(K^{(x)}|L)\tilde{\Gamma}^{KL} \quad (14)$$

For PP and IP, the effective two-particle density matrix is sparse. For PP, there is a linear number of nonzero terms: Γ_{iiii}, $\Gamma_{i^*i^*i^*i^*}$, $\Gamma_{iii^*i^*}$, $\Gamma_{ii^*i^*i}$, $\Gamma_{ii^*ii^*}$, and $\Gamma_{i^*i^*ii}$. For IP, there is a quadratic number of nonzero terms: Γ_{iijj}, Γ_{ijji}, $\Gamma_{iij^*j^*}$, $\Gamma_{ij^*j^*i}$, $\Gamma_{i^*i^*j^*j^*}$, $\Gamma_{i^*j^*j^*i^*}$, $\Gamma_{ii^*jj^*}$, $\Gamma_{ij^*ji^*}$, and $\Gamma_{i^*j^*ji}$. This significantly reduces both the storage and computational requirements of the above intermediates.

Here is a step-by-step description of the RI algorithm for the gradient with respect to auxiliary basis centers, with PP and then IP cost scalings indicated in parentheses where they differ (and assuming three-center integrals are left over from the PP/IP calculation):

1c. Compute: $(K^{(x)}|L)$ (X^2)

2c. Compute: $(K|L)^{-1}$ (X^3)

3c. Transform: $A^K_{\mu\nu} = \sum_L (K|L)^{-1}(L|\mu\nu)$ (NFP X^2)

4c. Transform: $A^K_{\mu q} = \sum_\nu A^K_{\mu\nu}C_{\nu q}$ (NFP $X\,o$)

5c. Transform: $A^K_{pq} = \sum_\mu A^K_{\mu q}C_{\mu p}$ ($N\,X\,o$, $N\,X\,o^2$)

6c. Contract: $\tilde{\Gamma}^K_{pq} = \sum_{rs}\Gamma_{pqrs}A^K_{rs}$ ($X\,o$, $X\,o^2$)

7c. Contract: $\tilde{\Gamma}^{KL} = \sum_{pq}A^K_{pq}\tilde{\Gamma}^L_{pq}$ ($X^2\,o$, $X^2\,o^2$)

8c. Compute: $(\mu\nu|K^{(x)})$ (NFP X)

9c. Transform: $(\mu q|K^{(x)}) = \sum_\nu (\mu\nu|K^{(x)})C_{\nu q}$ (NFP $X\,o$)

10c. Transform: $(pq|K^{(x)}) = \sum_\mu (\mu q|K^{(x)})C_{\mu p}$ ($N\,X\,o$, $N\,X\,o^2$)

11c. Increment/Contract: $\nabla E \leftarrow \sum_{pq,K}(pq|K^{(x)})\tilde{\Gamma}^K_{pq}$ ($X\,o$, $X\,o^2$)

12c. Increment/Contract: $\nabla E \leftarrow \sum_{KL}(K^{(x)}|L)\tilde{\Gamma}^{KL}$ (X^2)

Like for the RI algorithm for the PP/IP energy, the most expensive steps are transformation steps such as 4c, 5c, 9c, and 10c, for modestly large systems. Step 7c is the only new type of fourth-order step introduced, and this only for IP. In total, the calculation of the gradient is costlier than a single iteration of PP/IP, because of the prefactor introduced by transformations for each derivative component. Figure 1 shows a comparison of the required gradient and energy CPU

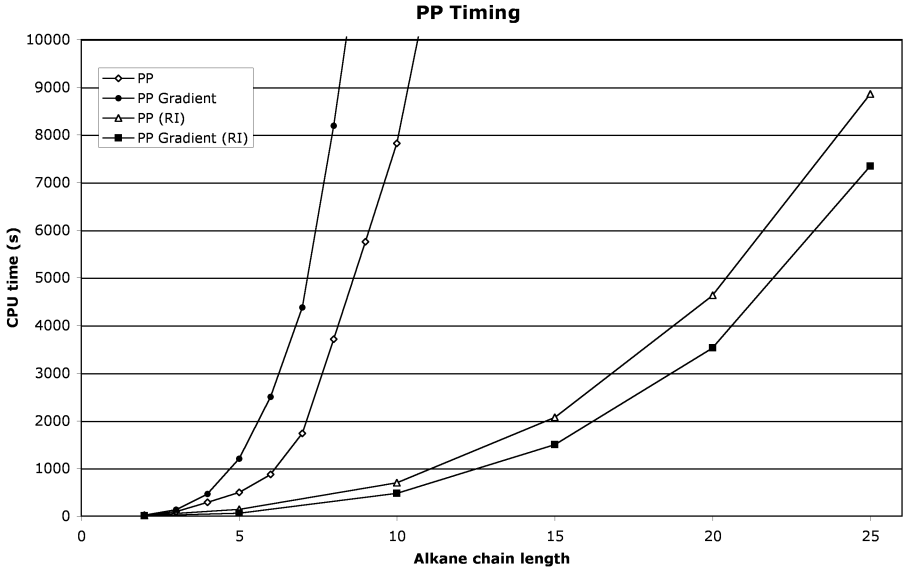

Figure 1. Total CPU time for a series of linear alkanes. Calculations were run on one 2.3 GHz Xserve G5 processor, with 8 GB of RAM, using a cc-pVDZ basis set and its corresponding RIMP2 fitting basis.[28]

time for a series of linear alkanes using the restricted perfect pairing method.

4. An Application of Imperfect Pairing: Prediction of Diradical Character

IP should provide an adequate description of strongly correlated systems, such as open-shell singlet diradicaloids.[30] Species with diradical character are important in that they may be intermediates in chemical reactions. It is also imaginable that they would be useful for their unique properties, in that they would have two weakly coupled unpaired electrons. One desires to apply a high-level correlated treatment to such problems, but stable diradicaloids are often only stable because of steric substituent effects, making calculations on all but the smallest model systems too costly for coupled-cluster doubles theory. As Kohn−Sham DFT,[31] through its representation as a single electron configuration, does not provide for correlated fractional occupation of orbitals except through spin-symmetry breaking, it is of limited use in diagnosing diradical character. As IP is based on coupled-cluster theory, its t amplitudes provide quantitative indications of partial virtual orbital occupation. Furthermore, our efficient implementation of IP has enabled us to explore a broader range of such molecules than before.

We applied the IP method to a model of a stable diradicaloid compound synthesized by Cui et al.[32] In forming the model, we kept a modestly sized portion of a very bulky substituent. The model molecule is shown in Figure 2. It is of a class of diradicaloids with a strained four-member ring, in which two diagonally opposed atoms (in this case, germaniums) have a partially filled valence. The calculation was performed with the SVP[29] basis, and with Ahlrichs' corresponding fitting basis.[12] The HOMO and LUMO calculated with IP are shown in Figure 2. The HOMO and LUMO appear to be out-of-phase nonbonding orbitals, consistent with Cui et al.'s DFT calculations, and also with a simple interpretation of germanium's valence. We found that the HOMO had a fractional occupation of 78.9% and

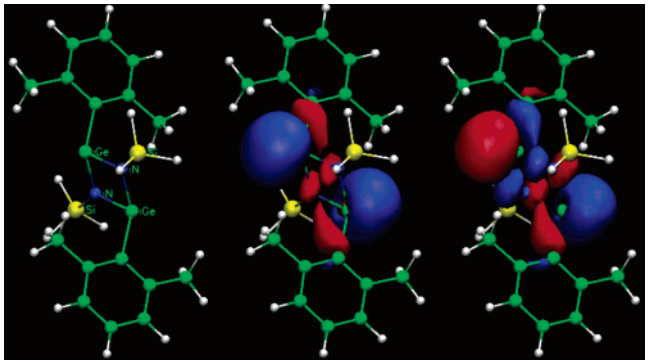

Figure 2. Left to right are the model molecule, the HOMO, and the LUMO.

that the LUMO had 21.1%. Considering the out-of-phase nature of the HOMO and LUMO, and what we consider a good definition of the measure of diradical character,[33] this indicates extremely high diradical character, as far as stable singlet diradicals go. If one imagines that a pure diradical would have 50% HOMO occupation and 50% LUMO occupation, consistent with an H_2 molecule with a stretched bond, 21.1% LUMO occupation means 42.2% diradical character. Although the pool of synthesized stable singlet diradicaloids available for comparison at this point in time is small, we would consider 42.2% diradical character to be quite remarkable. As a comparison, consider the very much reactive Si(100) surface. The cleaved surface rearranges to form Si dimers whose bonds are intermediate between a single and a double bond and which have about 35% diradical character,[34] less than that of Cui et al.'s stable singlet diradicaloid.

We must reiterate that we did not run IP on the full synthesized molecule and that the protective groups could have an important stabilizing effect and could increase the HOMO−LUMO gap, decreasing the diradical character. We will present a more thorough study of this stable singlet diradicaloid in a future work. Still, the IP method here serves to reaffirm the conclusion the authors made (that the

molecule was indeed a singlet diradicaloid), the evidence for which was a strained DFT geometry, spectroscopic data, and its reactivity. Here, IP adds an important indication of diradical character.

5. Conclusion

We have presented an efficient implementation of an RI algorithm for calculating the PP and IP energy, as well as the nuclear gradient for both PP and IP. The RI approximation eliminates the need for four-center two-electron integrals by replacing two-center atomic orbital function products with a sum of one-center auxiliary basis functions. This creates separability between the two electrons of the two-electron integral, allowing one to transform the two coordinates of the integral from an AO representation to an MO representation independently. While this introduces fourth-order scaling due to the RI contraction step, in the regime where PP and IP are feasible, it significantly reduces computational cost by about a factor of 10, while introducing error that is not likely to impact quantitative results. The speed of the method is then very much comparable to SCF theory, at least until linear scaling approximations for Fock matrix construction become useful.

As an example of a calculation readily feasible for PP and IP, yet far more costly for a full doubles treatment, such as CCD, we chose a model of a recently synthesized stable singlet biradical. Our correlated treatment of the system showed significant biradical character for the molecule, a result that DFT can only predict by inference through calculated structural properties.

Acknowledgment. This work was partly supported by the Department of Energy, Office of Basic Energy Sciences, SciDAC Computational Chemistry Program (Grant DE-FG0201ER403301), with additional support from subcontracts from National Institutes of Health Small Business Innovation Research Grants to Q-Chem Inc. M.H.-G. is a part-owner of Q-Chem Inc.

References

(1) Sklar, A. L. *J. Chem. Phys.* **1939**, *7*, 984−993.

(2) Mulliken, R. *J. Chem. Phys. Phys. Chim. Biol.* **1949**, *46*, 497.

(3) Løwdin, P. *J. Chem. Phys.* **1953**, *21*, 374−375.

(4) Harris, F. E.; Rein, R. *Theor. Chem. Acc.* **1966**, *6*, 73−82.

(5) Billingsley, F. P.; Bloor, J. E. *J. Chem. Phys.* **1971**, *55*, 5178−5190.

(6) Newton, M. D. *J. Chem. Phys.* **1969**, *51*, 3917−3926.

(7) Baerands, E. J.; Ellis, D. E.; Ros, P. *Chem. Phys.* **1973**, *2*, 41−51.

(8) Vahtras, O.; Almløf, J.; Feyereisen, M. W. *Chem. Phys. Lett.* **1993**, *213*, 514−518.

(9) Whitten, J. L. *J. Chem. Phys.* **1973**, *58*, 4496−4501.

(10) Dunlap, B. I.; Connolly, J. W. D.; Sabin, J. R. *J. Chem. Phys.* **1979**, *71*, 3396−3402.

(11) Eichkorn, K.; Treutler, O.; Øhm, H.; Häser, M.; Ahlrichs, R. *Chem. Phys. Lett.* **1995**, *240*, 283−289.

(12) Weigend, F.; Häser, M.; Patzelt, H.; Ahlrichs, R. *Chem. Phys. Lett.* **1998**, *294*, 143−152.

(13) Bernholdt, D. E.; Harrison, R. J. *J. Chem. Phys.* **1998**, *109*, 1593−1600.

(14) Beebe, N. H. F.; Linderberg, J. *Int. J. Quantum Chem.* **1977**, *12*, 683−705.

(15) O'Neal, D. W.; Simons, J. *Int. J. Quantum Chem.* **1989**, *36*, 673−688.

(16) Ten-no, S.; Iwata, S. *J. Chem. Phys.* **1996**, *105*, 3604−3611.

(17) Weigend, F. *Phys. Chem. Chem. Phys.* **2002**, *4*, 4285−4291.

(18) Bernholdt, D. E.; Harrison, R. J. *Chem. Phys. Lett.* **1996**, *250*, 477−484.

(19) Langlois, J.; Muller, R. P.; Coley, T. R.; Goddard, W. A., III; Ringnalda, M. W.; Won, Y.; Friesner, R. A. *J. Chem. Phys.* **1990**, *92*, 7488−7497.

(20) Cullen, J. *Chem. Phys.* **1996**, *202*, 217−229.

(21) Bobrowicz, F. W.; Goddard, W. A., III. *Modern Theoretical Chemistry: Methods of Electronic Structure Theory*; Schaefer, H. F., III, Ed.; Plenum: New York, 1977; Vol. 3, pp 79−126.

(22) Van Voorhis, T.; Head-Gordon, M. *J. Chem. Phys.* **2002**, *117*, 9190−9201.

(23) Van Voorhis, T.; Head-Gordon, M. *Chem. Phys. Lett.* **2000**, *317*, 575−580.

(24) Beran, G. J. O.; Austin, B.; Sodt, A.; Head-Gordon, M. *J. Phys. Chem. A* **2005**, *109*, 9183−9192.

(25) Krylov, A. I.; Sherrill, C. D.; Byrd, E. F. C.; Head-Gordon, M. *J. Chem. Phys.* **1998**, *109*, 10669−10678.

(26) Dunlap, B. I. *THEOCHEM* **2000**, *529*, 37−40.

(27) Kong, J. *J. Comput. Chem.* **2000**, *21*, 1532−1548.

(28) Weigend, F.; Køhn, A.; Hättig, C. *J. Chem. Phys.* **2002**, *116*, 3175−3183.

(29) Schäfer, A.; Horn, H.; Ahlrichs, R. *J. Chem. Phys.* **1992**, *97*, 2571−2577.

(30) Salem, L.; Rowland, C. *Angew. Chem., Int. Ed.* **1972**, *11*, 92−111.

(31) Kohn, W.; Becke, A. D.; Parr, R. G. *J. Phys. Chem.* **1996**, *100*, 12974−12980.

(32) Cui, C.; Brynda, M.; Olmstead, M. M.; Power, P. P. *J. Am. Chem. Soc.* **2004**, *126*, 6510−6511.

(33) Jung, Y.; Head-Gordon, M. *ChemPhysChem* **2003**, *4*, 522−525.

(34) Jung, Y.; Akinaga, Y.; Jordan, K. D.; Gordon, M. S. *Theor. Chem. Acc.* **2003**, *109*, 268−273.

CT050239B